Neutron-diffraction study of $Zr(Ca,Y)O_{2-x}$: Evidence of differing mechanisms for internal and external distortions

J. Faber, Jr. and M. H. Mueller

Argonne National Laboratory, Argonne, Illinois 60439

B. R. Cooper

Department of Physics, West Virginia University, Morgantown, West Virginia 26506
(Received 19 August 1977)

We have deduced from measurements of the neutron elastic cross section that below the order-disorder transition in $Zr(Ca)O_{2-x}$ and $Zr(Y)O_{2-x}$ the oxygen atoms are shifted from their fluorite positions. We find quantitative agreement with experiment for a model containing a rearrangement (internal shear deformation with amplitude 0.23 Å) of the oxygen sublattice. The (110) internal shear deformation is the same (in symmetry and magnitude) for $Zr(Ca)O_{2-x}$ and $Zr(Y)O_{2-x}$, however, only $Zr(Y)O_{2-x}$ exhibits an external distortion. These observations are consistent with the fact that the internal rearrangement is an inhomogeneous deformation and does not require the presence of an external strain. A successful test of Cooper's search criterion leads us to an internal rearrangement mode corresponding to a $\vec{q} = (0,0,2\pi/a)$ longitudinal phonon, and points to the dominance of cation-anion interactions in determining the nature of the lattice internal rearrangement.

I. INTRODUCTION

We report the observation of an internal distortion in $Zr(Ca)O_{2-x}$ and $Zr(Y)O_{2-x}$. This result is generically related to the earlier observation[1,2] of an internal distortion in UO_2 (a magnetic system). However, for $Zr(Ca)O_{2-x}$ and $Zr(Y)O_{2-x}$, the simplification is that exchange effects can be neglected. The unique feature of our observation is that an external strain is present only in $Zr(Y)O_{2-x}$. Thus, the external strain is not coupled to the internal distortion. This means that a minimum in the free energy is satisfied by coupling between the crystalline electric field and elastic energy that is essentially independent of the external strain. In the light of Cooper's search criterion,[3] we are led to infer that the internal rearrangement basically involves anion-cation (and indirectly, anion-anion) interactions and that the external strain in $Zr(Y)O_{2-x}$ principally involves cation-cation interactions.

Our present study has developed from the continuing interest[4-10] in the order-disorder transformation in $Zr(Ca, Y)O_{2-x}$. Neutron-diffraction studies of $Zr(Ca)O_{2-x}$ in the disordered and ordered state were first reported by Carter and Roth.[5] Above the transition (disordered state) the unit-cell symmetry is fcc fluorite ($Fm3m$), and they found in this state there is a displacement of the oxygen ions from the ideal fluorite lattice sites. The order-disorder transition occurs at ~1300 K and they inferred from their measurements that the ordered state involved cooperative ordering of the oxygen ions on the oxygen sublattice.

II. EXPERIMENT

Well-characterized single crystals of $Zr_{0.85}Ca_{0.15}O_{1.85}$ and $Zr_{0.82}Y_{0.18}O_{1.91}$ were used in our experiments. These crystals were heated at 1675 K to produce the disordered state or annealed at 1250 K for 400 h to obtain the ordered state. The Ca and Y concentrations were checked by x-ray fluorescence analysis. Neutron studies were carried out at the CP-5 research reactor on the full-circle diffractometer using a wavelength $\lambda = 1.05$ Å obtained in transmission from a Be monochromator ($\frac{1}{2}\lambda$ was minimized by the use of a Pu filter). Absorption corrections were made and only small extinction corrections were necessary. Our refinements for both crystals in the disordered state yielded results similar to those of Carter and Roth[5] for $Zr(Ca)O_{2-x}$ and Steele and Fender[11] for $Zr(Y)O_{2-x}$. Full details of our structural results and implications of our findings for transport properties will be published elsewhere.

The onset of ordering is apparent by a reduction in the symmetry of the lattice. For an fcc lattice (the disordered state), only reflections for which $h+k+l=4n$, $4n\pm1$, or $4n\pm2$, where n is an integer, are allowed. In the ordered state, forbidden reflections arise with h, k, and l mixed odd and even. In Fig. 1(a) we show the experimental values obtained for $Zr(Ca)O_{2-x}$. Only a particular subset of reflections occur such that h, $k=2n+1$, and $l=2n$. Furthermore, the intensities correlate with the l index. We anticipate[1,2,5,11] that the forbidden reflections arise from small (static) ordered displacements of the ions from their fluorite

equilibrium positions. However, an additional ex-
perimental constraint must be satisfied. Carter
and Roth[5] have studied the variation of the unit-
cell dimensions with the onset of the ordered state
using x-ray techniques (x-ray scattering is strong-
ly weighted towards effects on the metal sublattice,
since the atomic scattering factor $f_M \gg f_{Ox}$). For
$Zr_{0.85}Ca_{0.15}O_{1.85}$, they find that a change in dim-
ensions of the unit cell ($a = b = c$, $\alpha = \beta = \gamma = \frac{1}{2}\pi$) is
absent or extremely small ($\Delta a/a < 4 \times 10^{-5}$). Our
neutron experiments, while limited in instrument-
al resolution compared with x rays, could not de-
tect an external distortion (in contrast with the x-
ray case discussed above, the neutron experiments
have scattering lengths $b_M \sim b_{Ox}$ and are much more
sensitive to effects on the oxygen sublattice). The
consequence of these observations is that we may
restrict our search for a model to explain the ex-
perimental data that considers only oxygen sublat-
tice displacements. Moreover, the oxygen sublat-
tice displacements must *not* require attendant dis-
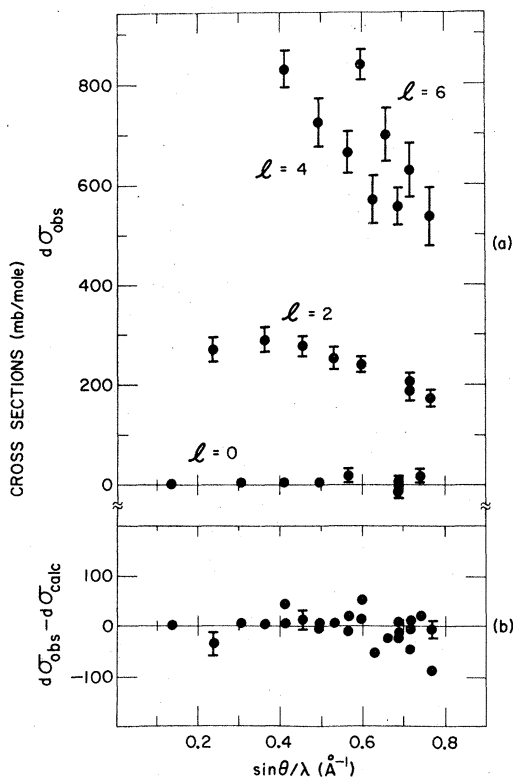placements of the metal atoms (the net force

FIG. 1. (a) Experimental values of the observed
cross section, $d\sigma_{obs}$ for $Zr(Ca)O_{2-x}$. In addition to the
parent fcc reflections (not shown), only reflections
with two odd and one even indices are observed. (b)
Residuals obtained after least-squares analysis using
Eq. (2). The model is illustrated in Fig. 3.

FIG. 2. (a) Experimental values of the observed cross
section for $Zr(Y)O_{2-x}$. In addition to the parent fcc re-
flections (not shown), only reflections with two odd and
one even indices are observed. (b) Residuals obtained
after least-squares analysis using Eq. (2). The model
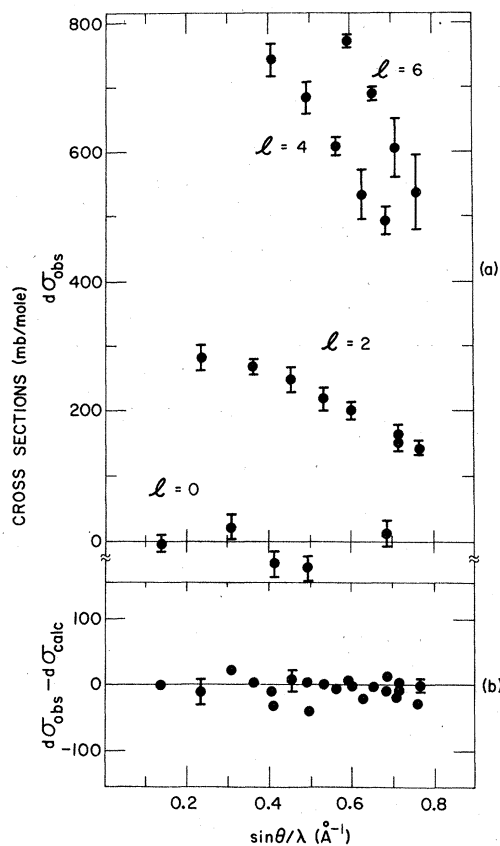is illustrated in Fig. 3.

summed at the metal atom positions must be zero).
Experimental values for the mixed reflections ob-
tained from the $Zr(Y)O_{2-x}$ single crystal are shown
in Fig. 2 (a). The similarity with the data shown
in Fig. 1 (a) is most striking. Apart from small
scaling differences the data in Figs. 1 (a) and 2 (a)
are identical. However, for $Zr(Y)O_{2-x}$ we find that
the dimensions of the unit cell are not cubic. The
fluorite unit cell is distorted tetragonally [c/a
$= 1.014(1)$] in the ordered state. In this case an
external strain is present.

III. ANALYSIS

To begin the analysis, we consider whether the
additional scattering present for the forbidden re-
flections shown in Figs. 1 (a) and 2 (a) arises from
small (static) displacements of the atoms from
their equilibrium positions. Local distortions of
the oxygen sublattice can be represented in terms
of the 27 displacement modes for a nine-atom as-

sembly consisting of one metal and eight cubic-coordinated oxygen atoms, and can be classified by their symmetry types. For the group O_h, the modes corresponding to distortions of the cube are

$$A_{1g} + E_g + 2T_{2g} + A_{2u} + E_u + 2T_{1u} + T_{2u}. \qquad (1)$$

In addition, there are T_{1u} (translation of the center of mass) and T_{1g} (rigid rotation) modes. Some of the distortional modes correspond to deformations of the two individual fcc oxygen sublattices, i.e., give external distortions (e.g., the two components of an E_g mode lead to tetragonal and orthorhombic unit cells[12]). Other distortional modes correspond to rigid shifts of the fcc oxygen sublattices, i.e., give internal distortions (e.g., one of the T_{2g} modes[12]). However, none of the modes of a single symmetry type, i.e., homogeneous deformations, as specified in Eq. (1) can explain the experimental data.

The absence of any appreciable external strain in $Zr(Ca)O_{2-x}$ and the failure of the individual normal modes to account for the neutron results lead us to consider inhomogeneous deformations, i.e., linear combinations of the normal modes. The deformation of this type that satifies the experimental behavior is shown in Fig. 3. This mode has $E_u + A_{2u}$ symmetry. To test this (110) oxygen sublattice shear deformation, we have performed a least-squares refinement with the quantities $d\sigma_{obs}$ of Figs. 1(a) and 2(a) as experimental input. The calculated cross section $d\sigma_{calc}$ arises from the oxygen displacements, and can be reduced to

$$d\sigma_{calc} = K\{b_0 \sin[2\pi l (\tfrac{1}{4} + \Delta/a)]\}^2$$

$$\times e^{-2W_0} Ay / \sin 2\theta \quad \text{mb/mole}, \qquad (2)$$

where K is an experimental scale factor, b_0 is the oxygen scattering length, Δ/a is the fractional displacement of the oxygen atom from the ideal fluorite lattice site, $W_0 = B_0 \sin^2 \theta / \lambda^2$ is the Debye-Waller factor for the oxygen atoms, A is the absorption factor, y is the extinction factor, and 2θ is the scattering angle.

Three adjustable parameters were used in the least-squares fit: K, B_0, and Δ. For $Zr(Ca)O_{2-x}$, 25 independent reflections (resulting from 250 observations) were obtained, and Eq. (2) provides an excellent fit as illustrated by plotting the point by point residuals in Fig. 1(b). The agreement factor $(\sum |d\sigma_{obs} - d\sigma_{calc}| / \sum d\sigma_{obs})$ is 0.058 and $\chi^2 = 0.92$ for this fit. The internal rearrangement mode is shown in Fig. 3. For $Zr(Y)O_{2-x}$, 22 independent reflections (resulting from 280 observations) were obtained, and the point by point residuals for this fit are illustrated in Fig. 2(b), again using the
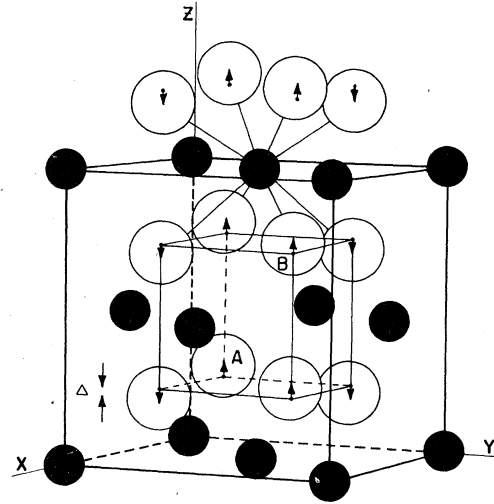

FIG. 3. Cubic fcc fluorite unit cell. The solid circles are the cations at 000+fcc translations. The open circles are the anions at fractional unit-cell coordinates $\tfrac{1}{4}$, $\tfrac{1}{4}$, $\tfrac{1}{4}$ (atom labeled A) and $\tfrac{3}{4}$, $\tfrac{3}{4}$, $\tfrac{3}{4}$ (atom labeled B). The upper portion of the figure defines a nine-atom assembly for use with Eq. (1). The oxygen atoms are displaced from their ideal fluorite lattice sites in directions shown by the arrows. The fractional shift of the oxygen atoms, $\Delta/a = 4.4 \times 10^{-2}$, is not drawn to scale.

mode illustrated in Fig. 3. The agreement factor for this fit is 0.021 and $\chi^2 = 0.85$. The parameter of interest is Δ/a, the fractional coordinate shift of the oxygen atom from its ideal fluorite position. The least-squares fits gave $\Delta/a = (4.4 \pm 0.1) \times 10^{-2}$, which satisfied the data in Figs. 1 (a) and 2 (a) equally well. The shift in the oxygen position is 0.23 Å. The deformation in Fig. 3 does not contribute to the reciprocal lattice points with h, $k = 2n$ and $l = 2n + 1$.

IV. LATTICE INTERNAL-REARRANGEMENT MODES

Thus, considering inhomogeneous deformations, we have introduced an internal rearrangement mode, of symmetry $E_u + A_{2u}$ (considered as a normal mode of the nine-atom assembly consisting of a cation in its "cage" of eight nearest-neighbor anions) as illustrated in Fig. 3, that quantitatively accounts for the neutron intensities from $Zr(Ca)O_{2-x}$ and $Zr(Y)O_{2-x}$. Lattice internal rearrangement modes are modes that distort one sublattice in some periodic way, while leaving the atoms of another sublattice at their undistorted positions. Cooper[3] has developed a search criterion for lattice internal rearrangement modes. To discuss our results in the context of this theory, let us turn to a summary of the detail relevant to

fluorite structure materials.

The search criterion[3] involves the ansatz that the internal rearrangement mode that occurs is least unfavorable with respect to an increase in elastic energy. Elastic equilibrium is maintained for the undistorted sites, i.e., the assumption is made that the net elastic force on the undistorted sites vanishes under the action of an internal rearrangement, just as it does in the undistorted crystal. Together with this ansatz, the search criterion requires a model for the elastic forces. Cooper considered only short-range radial elastic forces. Since we shall restrict our attention to modes with wave vector $\vec{q}$ at high-symmetry points in the Brillouin zone, the modes are principally determined by symmetry and not by the particular details of the elastic force model used.

For the fluorite structure, there are two kinds of anion sites, denoted by A and B, and the elastic force equations involve anion-cation Hook's law constants γ_{AC} and γ_{BC}. From physical considerations, we expect $\gamma_{AC} = \gamma_{BC} = \gamma$. Moreover, based on the experimental results, the cation sites are considered fixed. The condition of zero elastic force at the cation sites gives (with anion displacements $\vec{U}^{A,B} = \vec{\overline{U}}^{A,B} \exp[i(\vec{q} \cdot \vec{r} + \delta)]$) for $\vec{q} \| \langle 001 \rangle$,

$$0 = -\tfrac{8}{3}\gamma \cos(\tfrac{1}{4}qa)U_{qx}^A - \tfrac{8}{3}\gamma \cos(\tfrac{1}{4}qa)U_{qx}^B, \qquad (3a)$$

$$0 = -\tfrac{8}{3}\gamma \cos(\tfrac{1}{4}qa)U_{qy}^A - \tfrac{8}{3}\gamma i \sin(\tfrac{1}{4}qa)U_{qz}^A$$
$$-\tfrac{8}{3}\gamma \cos(\tfrac{1}{4}qa)U_{qy}^B + \tfrac{8}{3}\gamma i \sin(\tfrac{1}{4}qa)U_{qz}^B, \qquad (3b)$$

$$0 = -\tfrac{8}{3}\gamma i \sin(\tfrac{1}{4}qa)U_{qy}^A - \tfrac{8}{3}\gamma \cos(\tfrac{1}{4}qa)U_{qz}^A$$
$$+\tfrac{8}{3}\gamma i \sin(\tfrac{1}{4}qa)U_{qy}^B - \tfrac{8}{3}\gamma \cos(\tfrac{1}{4}qa)U_{qz}^B. \qquad (3c)$$

There are two types of solutions: either (i) $\vec{q} = (0, 0, 2\pi/a)$, $U_{qx}^A = U_{qx}^B$, and $U_{qy}^A = U_{qy}^B$, or (ii) $U_{qz}^A = -U_{qz}^B$ and $U_{qy}^A = U_{qy}^B = U_{qx}^A = U_{qx}^B = 0$. Thus we see that the constraint of zero force at the undistorted sites is very restrictive, and the search criterion leads to quite specific predictions concerning the wave vector and polarization of the lattice internal rearrangement modes that will occur.

For the first solution, $\vec{q}$ is completely determined to be $(0, 0, 2\pi/a)$. The transverse mode of this type is the internal rearrangement mode observed[1] in UO$_2$. It is interesting to note that for $\vec{q} \| \langle 110 \rangle$, the zero cation force equations can only be satisfied for $\vec{q} = 0$ and $U_{qz}^A = -U_{qz}^B$. This is the internal strain (a homogeneous deformation with T_{2g} symmetry) predicted by Allen[12] to occur in UO$_2$. For $\vec{q} = (0, 0, 2\pi/a)$, the longitudinal mode with $U_{qz}^A = -U_{qz}^B$ [the solution satisfying both conditions (i) and (ii)] is the internal rearrangement mode that we observe in Zr(Ca)O$_{2-x}$ and Zr(Y)O$_{2-x}$. That

is, this normal mode of the crystal gives the behavior shown in Fig. 3 for the corresponding mode of the nine-atom assembly.

The observation of an internal distortion (identical in symmetry and magnitude) in Zr(Ca)O$_{2-x}$ *and* Zr(Y)O$_{2-x}$ and the appearance of an external strain (characterized by $c/a = 1.014$) *only* in Zr(Y)O$_{2-x}$ leads us to conclude that the internal distortion (Fig. 3) occurs without significant coupling to the external strain. In the context of Cooper's theory,[3] the occurrence of an internal rearrangement mode, with fixed cation sites, depends on a relatively large cation-cation interaction compared to other elastic interactions. Details of the internal rearrangement behavior depend on the cation-anion, and indirectly, on the anion-anion interaction. One then expects that an external strain occurs as the relative size of the cation-cation elastic interaction decreases. This picture leads us to suggest that an understanding of the external strain in Zr(Y)O$_{2-x}$ principally involves cation-cation interactions.

V. SUMMARY AND DISCUSSION

We have reported the observation of an internal rearrangement of the oxygen sublattice in the ordered state for Zr(Ca)O$_{2-x}$ and Zr(Y)O$_{2-x}$. In Sec. III, it was shown that (i) a description of the effect leads us to consider linear combinations of the normal modes (irreducible representations) of the undistorted lattice, (ii) a mode with $E_u + A_{2u}$ symmetry satisfies the experimental data for Zr(Ca)O$_{2-x}$ and Zr(Y)O$_{2-x}$, and (iii) the magnitude of the anion displacement is independent of the presence of an external strain. In Sec. IV, we have seen that the oxygen sublattice internal rearrangement is the result of a zone boundary, $\vec{q} = (0, 0, 2\pi/a)$ longitudinal mode. The phase of the displacement wave is π between anion sublattices. An important result is that an oxygen sublattice internal distortion can occur without the manifestation of an external strain. Moreover, a description of the oxygen sublattice internal rearrangement requires a consideration of only anion-cation (and indirectly, anion-anion) interactions.

Our conclusions suggest the need for several additional experiments. The elastic neutron-scattering experiments reported here involve dopant ions that stabilize the fluorite structure. However, these ions have different ionic charge and size (Ca^{2+} has $r_0 \sim 1$ Å, while Y^{3+} has $r_0 \sim 0.9$ Å). We are currently measuring the elastic scattering from Zr(Mg^{2+})O$_{2-x}$ ($r_0 \sim 0.7$ Å), to obtain additional information on the occurrence of an external strain and the magnitude of the internal distortion. Our elastic scattering experiments have identified the

mode of the internal distortion. The close correspondence between the zone boundary, $\vec{q} = (0, 0, 2\pi/a)$ internal rearrangement mode and its phonon analogy, suggests the need for an *inelastic* neutron experiment to search for the associated dynamic effects near the transition (a difficult experiment at the temperatures of interest). An elastic experiment on NpO_2 (a nonmagnetic[13] fluorite structure compound) has been suggested,[2] and in light of our present results, seems eminently worthwhile. The consequence of our observations for other magnetic compounds[3,14,15] with the NaCl structure suggest a number of experiments.

[1] J. Faber, Jr., G. H. Lander, and B. R. Cooper, Phys. Rev. Lett. **35**, 1770 (1975); *Magnetism and Magnetic Materials—1975*, edited by J. J. Becker, G. H. Lander, and J. J. Ryne (AIP, New York, 1976), p. 379.

[2] J. Faber, Jr. and G. H. Lander, Phys. Rev. B **14**, 1151 (1976).

[3] B. R. Cooper, Phys. Rev. B **17**, 293 (1978).

[4] T. Y. Tien and E. C. Subbarao, J. Chem. Phys. **39**, 1041 (1963).

[5] R. E. Carter and W. L. Roth, *Electromotive Force Measurements in High-Temperature Systems*, edited by C. R. Alcock (American Elsevier, New York, 1968), p. 125.

[6] T. H. Etsell and S. N. Flengas, Chem. Rev. **70**, 339 (1970).

[7] J. G. Allpress, H. J. Rossell, and H. G. Scott, J. Solid State Chem. **14**, 264 (1975); J. G. Allpress and H. J. Rossell, *ibid.*, **15**, 68 (1975).

[8] B. Hudson and P. T. Moseley, J. Solid State Chem. **19**, 383 (1976).

[9] G. Bacquet, J. Dugas, and C. Escribe, J. Solid State Chem. **19**, 251 (1976).

[10] V. G. Keramidas and W. B. White, J. Phys. Chem. Solids **34**, 1873 (1973).

[11] D. Steele and B. E. F. Fender, J. Phys. C **7**, 1 (1974).

[12] Modes with E_g and T_{2g} symmetry are described pictorially in Ref. 1 and in S. J. Allen, Phys. Rev. **166**, 530 (1968).

[13] B. D. Dunlap, G. M. Kalvius, D. J. Lam, and M. B. Brodsky, J. Phys. Chem. Solids **29**, 1365 (1968).

[14] K. W. H. Stevens and E. Pytte, Solid State Commun. **13**, 101 (1973).

[15] G. H. Lander and M. H. Mueller, Phys. Rev. B **10**, 1994 (1974).